ACS APPLIED MATERIALS & INTERFACES

Research Article

www.acsami.org

Orientation-Dependent Electronic Structures and Charge Transport Mechanisms in Ultrathin Polymeric n-Channel Field-Effect Transistors

Simone Fabiano,[†,‡] Hiroyuki Yoshida,[*,§,⊥] Zhihua Chen,[∥] Antonio Facchetti,[*,∥] and Maria Antonietta Loi[*,‡]

[‡]Zernike Institute for Advanced Materials, University of Groningen, Nijenborgh 4, 9747 AG Groningen, The Netherlands

[§]Institute for Chemical Research, Kyoto University, Uji, Kyoto 611-0011, Japan

[⊥]PRESTO, Japan Science and Technology Agency, 4-1-8 Honcho Kawaguchi, Saitama 332-0012, Japan

[∥]Polyera Corporation, Skokie, Illinois 60077, United States

ABSTRACT: We investigated the role of metal/organic semiconductor interface morphology on the charge transport mechanisms and energy level alignment of the n-channel semiconductor poly{[N,N′-bis(2-octyldodecyl)-naphthalene-1,4,5,8-bis(dicarboximide)-2,6-diyl]-alt-5,5′-(2,2′-bithiophene)} (P(NDI2ODT2)). Variable-temperature study of well-ordered edge-on-oriented P(NDI2OD-T2) monolayer and multilayer field-effect transistors fabricated via Langmuir−Schäfer (LS) method reveals a higher activation energy for the edge-on morphology when compared to that extracted for the face-on oriented P(NDI2OD-T2) spin-coated films, which showed a weaker temperature dependence. Near-ultraviolet inverse photoemission and low-energy electron transmission spectroscopies are utilized to study these microstructurally defined polymeric films. The cross correlations of these techniques with the device characterization reveals the role of the molecular orientation at the semiconductor/contact interface in shifting the charge injection barrier. Finally, we demonstrate that the injection barrier for electrons is higher for the LS/edge-on than in the spin-coated/face-on films.

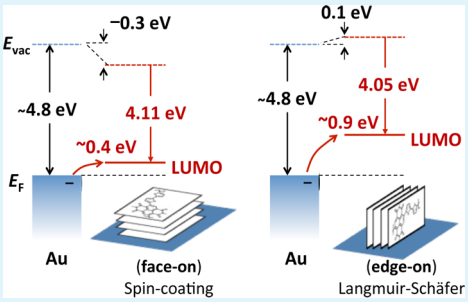

KEYWORDS: *field-effect transistor, conjugated polymer, monolayer, inverse photoemission spectroscopy, electron affinity, injection barrier*

INTRODUCTION

Organic field-effect transistors (OFETs) have attracted considerable attention because of their potential applications in unconventional electronics.[1−3] Because of their mechanical flexibility and facile processing, polymeric semiconductors are particularly suitable for fulfilling cheap processing requirements. Advancements in this field have been primarily stimulated by the discovery of new high-mobility materials;[4−8] nevertheless, a comprehensive understanding of the role of semiconductor interface morphology on the charge transport mechanisms remains relatively unexplored. For instance, it is well-established that the degree of structural order in organic thin film transistors affects the charge transport.[9−12] In particular, in a π-conjugated polymer with flexible solubilizing side chains such as regioregular poly(3-hexylthiophene) (rr-P3HT), charge transport is facile between stacked backbones, but poor when the alkyl side chains are in between the stacked main chains.[13] Moreover, recent surface science experiments have underlined the importance of the semiconductor film microstructure at the interface with the metallic electrodes, emphasizing the role of the molecular orientation at such an interface in shifting the charge injection barrier.[14−16] Several authors have also described that molecular dipoles (self-assembled) can shift the metal work function.[17] The alignment of the work-function of the source/drain metal with the energy levels of the semiconductor determines the efficiency of the charge injection. When analyzing the complex interplay between the molecular orientation at the interface and charge injection, one of the important physical parameters often missing is the precise value of electron affinity of the active layer, thus an accurate analysis of the semiconductor electronic structure in the proximity of the charge injecting contact. Unfortunately, because of the semiconducting polymer nature showing low degree of (long-range) order, it has been extremely difficult to study so far nondisordered interfaces between polymers and metals as well as investigating polymer monolayers as field effect transistor active layer.

Very recently, we have demonstrated n-channel mono/multilayer OFETs based on poly{[N,N′-bis(2-octyldodecyl)-naphthalene-1,4,5,8-bis(dicarboximide)-2,6-diyl]-alt-5,5′-(2,2′-bithiophene)} (P(NDI2OD-T2), Polyera ActivInk N2200) (Figure 1a), having a precise edge-on conformational order obtained via Langmuir−Schäfer (LS) deposition.[18] This deposition technique allows to obtain highly reproducible monolayer OFETs displaying high performances in a top-gate architecture using PMMA as dielectric. Our findings clearly

Received: March 2, 2013
Accepted: May 1, 2013
Published: May 1, 2013

   dx.doi.org/10.1021/am400786c | *ACS Appl. Mater. Interfaces* 2013, 5, 4417−4422

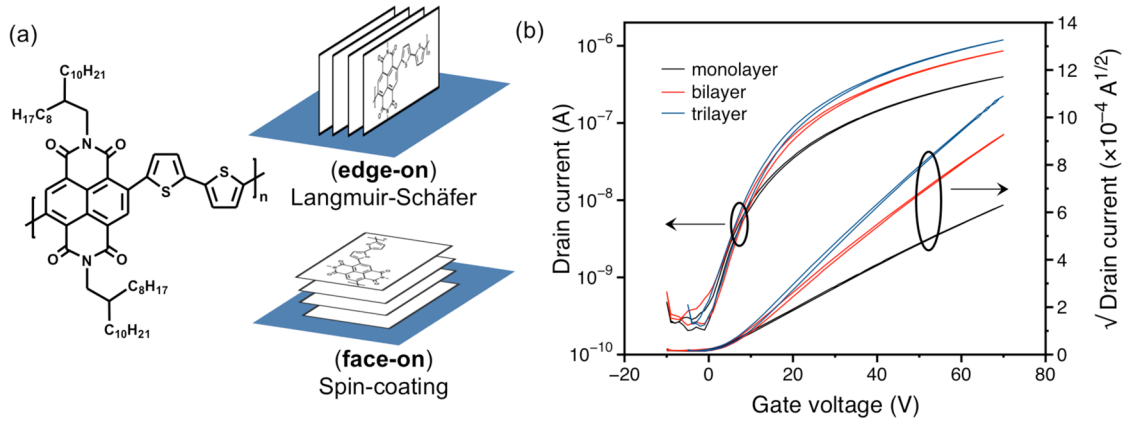

Figure 1. (a) Molecular structure of P(NDI2OD-T2). The film texture changes from edge-on (Langmuir–Schäfer deposition) to face-on (spin-coating). (b) Saturation transfer characteristics of LS-deposited monolayer, bilayer and trilayer P(NDI2OD-T2) OFETs at V_{DS} = 60 V (L = 50 μm, W = 500 μm).

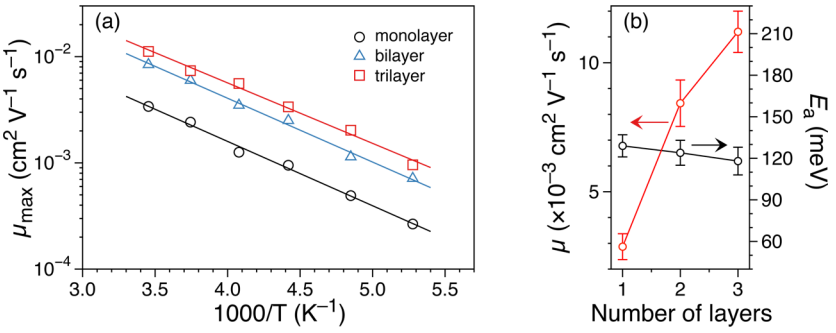

Figure 2. (a) Semilog plot of OFET mobility vs $1/T$ in the range 190–290 K for monolayer, bilayer and trilayer P(NDI2OD-T2) OFETs at V_{DS} = 60 V (L = 50 μm, W = 500 μm). The solid lines are least-squares fits to the Arrhenius relationship. (b) Electron mobility and activation energy as a function of the number of layers.

pointed out mobility anisotropies reflecting different polymer organization when OFETs were fabricated with LS multilayers (i.e., number of layers = 1–15) versus OFETs fabricated with spin-coated films. In the latter devices, the polymer was found to adopt a predominantly face-on (out-of-plane π-stacking) orientation[19] (Figure 1a) with a very high degree of aggregation,[20] which leads to a three-dimensional charge transport and hence electron mobility up to 1 order of magnitude larger than those measured for the LS/edge-on multilayer counterpart.[18] Large out-of-plane electron mobility has also been revealed by means of bulk electron transport measurements in face-on oriented P(NDI2OD-T2) films, showing the three-dimensional character of the charge transport in spin-coated films.[21] Moreover, recent studies addressed details of P(NDI2OD-T2) film microstructure and how this affects the device performances.[22]

In the present study, we aim at correlating the molecular orientation of the P(NDI2OD-T2) backbone with the corresponding electron transport properties and their evolution with the film thickness (number of LS layers) by means of variable-temperature electrical measurements. Our results reveal a thermally activated hopping transport with an activation energy of ~120 meV regardless of the number of LS layers. Interestingly, the activation energy is found to be higher than the one extracted for the face-on oriented P(NDI2OD-T2) films fabricated by spin-coating. Furthermore, measurements of the electron affinity by near-ultraviolet inverse photoemission and low-energy electron transmission spectroscopies revealed that the injection barrier for electrons is higher for the layered edge-on films than for the face-on ones. This result demonstrates that the larger mobilities measured for the spin-coated/face-on oriented P(NDI2OD-T2) films reflects not only efficient interchain transport in the three dimensions, as previously postulated,[18] but also a more favorable charge injection from the gold electrode.

RESULTS AND DISCUSSION

Top-gate bottom-contact OFETs were fabricated as described in the Experimental Methods. Briefly, glass slides with prepatterned Cr/Au contacts (L = 50 μm, W = 500 μm) were functionalized with hexamethyldisilazane (HMDS) and used as substrates. Monolayer and multilayers of P(NDI2OD-T2) were transferred by LS deposition and then thermally annealed in a vacuum oven overnight to fully remove the water. Although the molecular orientation of conjugated polymer spin-coated on Au electrodes can typically differ from that in the channel because of the attractive forces between the polymer and the gold, resulting in amorphous and random morphology on the electrodes,[23] it is worth noting that in the case of LS films, the out-of-plane molecular order of P(NDI2OD-T2) mono/multilayers is reached at the air/water interface during compression because of the π–π interactions between the aromatic backbones and the van der Waals interactions between the branched octyl-decyl side chains that promote the self-assembly in ordered close-packed forms. The films are thereby transferred to the substrate showing morphology and orientation that are independent of

the substrate surfaces.[18] The deposition of PMMA as gate dielectric and silver as gate electrode completed the field-effect transistors. Electrical measurement were performed at room temperature in vacuum. Layered P(NDI2OD-T2) OFETs show very good n-channel behavior, with transfer curves characterized by a very low hysterisis (Figure 1b). The typical maximum electron field-effect mobilities extracted for the mono-, bi-, and trilayer P(NDI2OD-T2) OFETs are in the range of 0.3−2 × 10^{-2} cm^2 V^{-1} s^{-1} in the saturation regime (V_{DS} = 60 V), in agreement with our previous results (see Figure 2b).[18] In addition, threshold voltages near zero and on/off current ratios larger than 10^3 are measured. Although the measured on/off current ratios are lower than those reported for p-type semiconductors typically of up to 10^6,[24] they are well within the high performance range reported previously for top-gated P(NDI2OD-T2) devices.[18,25] The contact resistance for the two different molecular orientations was measured by means of the differential method in the linear regime (V_{DS} = 5 V).[26] A contact resistance of about 0.2 MΩ cm was extracted for the face-on oriented P(NDI2OD-T2) OFETs while a contact resistance up to 1 order of magnitude higher (R_c = 1.2 MΩ cm) is derived for the edge-on oriented devices.

To investigate the charge transport in more detail, we performed temperature-dependent mobility measurements in both LS layered and spin-coated P(NDI2OD-T2) OFETs. All devices were first characterized by measuring the transfer characteristics at room temperature (RT) and then remeasured at temperature steps down to the lowest temperatures. The electron mobilities have been extracted from variable-temperature transfer curves using the standard equation valid for transistors in the saturation regime. The mobility decreases with temperature (Figures 2a and 3), as is usual in the case of

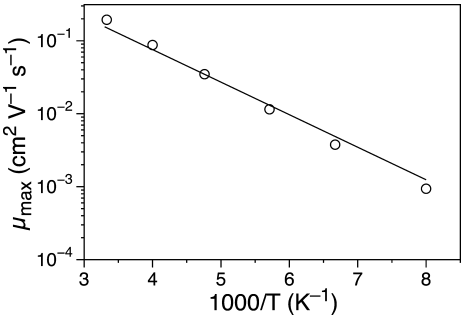

Figure 3. Semilog plot of OFET mobility vs $1/T$ in the range 125−300 K for spin-coated P(NDI2OD-T2) OFETs. The solid line is least-squares fit to the Arrhenius relationship showing an activation energy of ∼85 meV.

polymeric semiconductors, indicating temperature-activated hopping transport or charge injection.[27] An Arrhenius-like dependence of the mobility is observed ($\mu_{FET} \propto \exp(-E_a/kT)$), from which the activation energy (E_a) can be extracted. In literature, thermally activated mobility with activation energy of 80−90 meV has been shown for oligothiophene monolayers, and ascribed to hopping or trap-limited transport mechanism due to grain boundaries.[28,29] Variable-temperature mobility analyses of polymeric monolayer/multilayer OFETs have never been reported, because of the lower processability of polymers into highly ordered monolayers. Remarkably, although the electron mobility is found to increase going from monolayer to trilayer OFETs (Figure 2b), as demonstrated in our previous work,[18] we found that the activation energy for layered P(NDI2OD-T2) amounts to ∼120 meV regardless of the number of layers. This value of E_a is higher than that extracted for the spin-coated/face-on oriented P(NDI2OD-T2) films (thickness ∼50 nm), which showed a weaker temperature dependence (∼85 meV, Figure 3) and electron mobilities up to 1 order of magnitude higher (∼0.1 cm^2 V^{-1} s^{-1}). It has been shown for several organic semiconductors that an empirical correlation exists between mobility and activation energy. In particular, higher mobility polymers tend to exhibit lower activation energy.[30] P3HT-based OFETs having $\mu \approx 0.1$ cm^2 V^{-1} s^{-1} (edge-on orientation) typically exhibit E_a = 85 meV,[13,27] whereas higher activation energies (i.e., ∼115 meV) have been reported for $\mu \approx 2 \times 10^{-4}$ cm^2 V^{-1} s^{-1} (face-on orientation).[13] Similar activated behavior has been observed for poly(2,5-bis(3-tetradecylthiophen-2-yl)thieno[3,2-b]-thiophene) (pBTTT)-based OFETs with E_a = 83 meV for devices with $\mu \approx 0.1$ cm^2 V^{-1} s^{-1}.[31]

The weak temperature dependence for face-on oriented P(NDI2OD-T2) bulk film was explained in terms of low energetic disorder in this material.[32] The fact that the activation energy for the LS layered films, which we demonstrated to be very compact and characterized by a long-range order, is higher than the one measured for the less ordered face-on films could also be explained in terms of a lower charge injection. In fact, charge carriers need to overcome a larger injection barrier, a process that is known to be temperature-dependent, as from the thermionic emission model.[33] Different molecular orientations of the P(NDI2OD-T2) in the proximity of the metal contact have been reported to rise the injection barrier of about 300 meV leading to a larger activation energy.[34] The temperature dependence of charge injection rather than (or in addition to) the temperature dependence of hopping transport would explain why the activation energy of the edge-on oriented films is independent of the number of layers, whereas the electron mobility increases with the layer thickness. Indeed, if electron traps or hopping transport were the only source of the observed temperature-dependent mobility, we would expect a larger E_a with increasing the grain boundaries (increasing the number of layers). We believe that these results are indicative of both large contact resistance and intrinsic mobility anisotropy, deriving from the different organization of the polymer chains in the two cases. In particular, the effect of the long alkyl chain of the polymer in the LS/edge-on morphology may hinder the transport from one monolayer to the other.

To better rationalize the behavior of the LS/edge-on oriented P(NDI2OD-T2) films at the interface with the metal contact, it is important to investigate the electronic structure of this polymer in more details. Thus, we carried out accurate measurements of the LUMO levels of our films by inverse photoemission spectroscopy (IPES).[35−37] Because the cross-section of IPES is extremely low, high electron fluxes with kinetic energy around 10 eV are required, resulting generally in a radiation damage of the organic materials. In particular, the alkyl-chains are known to be very sensitive at these conditions,[38] therefore, it has been difficult so far to derive reliable information from the IPES of polymeric samples. Recently, inverse photoemission spectroscopy in the near-ultraviolet range (NUV-IPES) has been demonstrated, using electrons with kinetic energy below the damage threshold of organic materials.[39] Because our NUV-IPES set up is working in transmission configuration, optically transparent conductive substrates such as indium tin oxide (ITO) were employed. This

new technique is applied here to study the LUMO level energies of P(NDI2OD-T2) films with different orientations as shown in Figure 4.

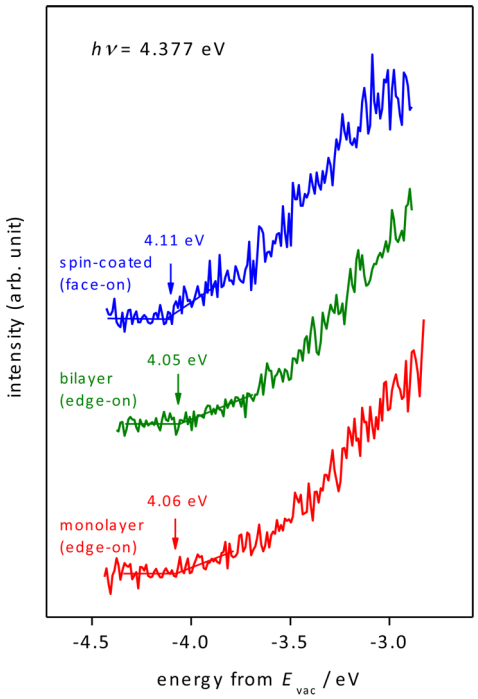

Figure 4. NUV-IPES spectra of LS mono- and bilayers of P(NDI2OD-T2) as well as a spin-coated P(NDI2OD-T2) film on HMDS-treated ITO.

The LUMO level of edge-on and face-on oriented P(NDI2OD-T2) films were first investigated on HMDS-modified ITO electrode, then the results were correlated with the vacuum level shift for a Au/P(NDI2OD-T2) interface, as measured by Kelvin Probe.

The NUV-IPES spectrum of HMDS displays no features (data not shown), whereas the one relative to the edge-on P(NDI2OD-T2) monolayer shows a variation of slope around 4.06 eV (Figure 4). By adding a second molecular layer of P(NDI2OD-T2), the NUV-IPES spectrum closely resembles the one measured for the monolayer, with an electron affinity (onset energy of the LUMO-derived feature with respect to the vacuum level) value of 4.05 eV. Interestingly, these values are close to those measured for spin-coated/face-on oriented P(NDI2OD-T2) films (i.e., 4.11 eV), and are in good agreement with the previous estimation performed by cyclic voltammetry,[40] but intrinsically more reliable and accurate.

Next, we investigated the same films on Au-coated glass substrates to match the OFET electron-injection device architecture. The electron injection barrier at the electrode is affected by the potential difference between the Au and P(NDI2OD-T2), known as the vacuum level shift, as well as the electron affinity of polymer layer and the work-function of metal. The vacuum level shift is generally assumed to derive from the push-back effect, charge transfer, chemical interaction between the metal and the adsorbate, and orientation of polar molecule.[41] Because the work-function of Au is in the range between 4.7 and 5.1 eV, the Fermi level of Au electrode falls near the middle of the energy gap of P(NDI2OD-T2), thus charge transfer between the Au and P(NDI2OD-T2) interfaces should be negligible.[42,43] Moreover, the chemical interaction between Au and the polymer is more unlikely. Although the P(NDI2OD-T2) polymer does not exhibit a fixed dipole moment, recent studies pointed out that the magnitude of the interface dipole layer is also affected by the orientation of nonpolar molecules.[15]

To examine the effect of the polymer backbone orientation on the vacuum level shift, the low-energy electron transmission (LEET) spectroscopy of both the spin-coated and LS films on HMDS-treated ITO was carried out and is shown in Figure 5.

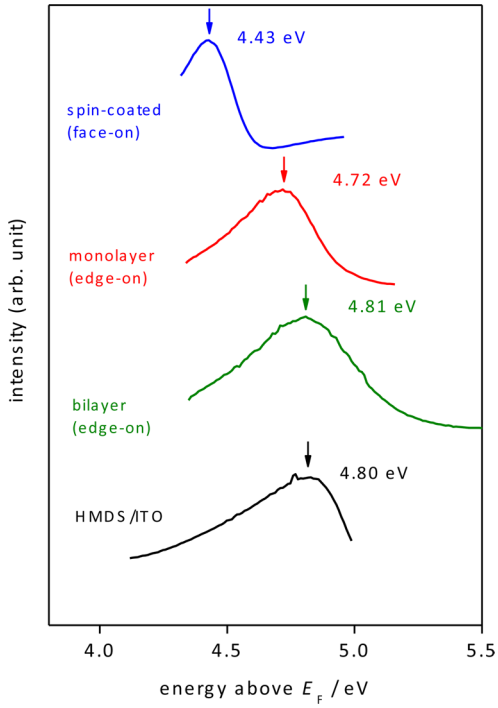

Figure 5. LEET spectra of the HMDS-treated indium tin oxide, the mono-, bi-, and spin-coated layers of P(NDI2OD-T2) on HMDS-treated ITO.

The vacuum level for the spin-coated layer is measured to be 4.43 eV, whereas the LS monolayer and bilayer have their vacuum levels at 4.72 and 4.81 eV, respectively. Note that, the difference in the vacuum levels between the mono- and bilayer is well within the experimental uncertainties, leading to a difference between face-on and edge-on vacuum levels of about 0.4 eV. The magnitude of 0.4 eV for the orientation-dependence measured on the HMDS-treated ITO substrate should be similar to that on the Au substrates. In fact, we assume that the surface dipole layer would not depend on the substrate, which is a reasonable assumption. The vacuum level shift for the LS/edge-on film is estimated as +0.1 eV, whereas is −0.3 eV for the spin-coated/face-on P(NDI2OD-T2) measured by Kelvin Probe method (KP).

Figure 6 shows the energy level diagram of the Au/P(NDI2OD-T2) interface derived from the NUV-IPES, LEET, and KP results. The ionization energy for the spin-coated P(NDI2OD-T2) is taken from ref.[43] Assuming that the work-function of Au is 4.8 eV, the electron injection barrier from the Au to the spin-coated/face-on P(NDI2OD-T2) is 0.4 eV, whereas it is 0.9 eV in case of the LS/edge-on P(NDI2OD-T2). Recent work on P3HT suggested that the magnitude of the interface dipole layer depends on the orientation of the

dx.doi.org/10.1021/am400786c | ACS Appl. Mater. Interfaces 2013, 5, 4417−4422

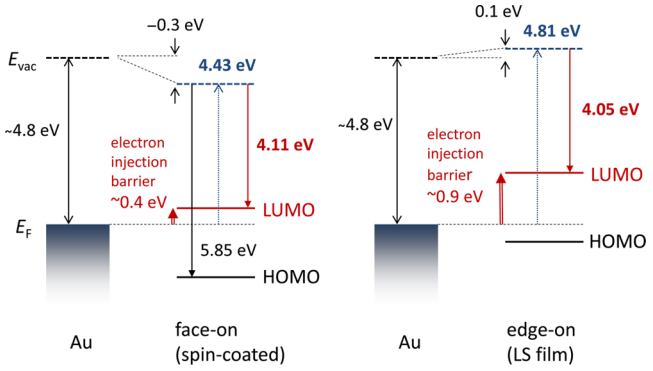

Figure 6. Energy level diagram of the Au and P(NDI2OD-T2) interface. The ionization energy of P(NDI2OD-T2) is taken from ref 43, whereas all the other values have been experimentally measured in this work.

polymer backbone.[15] The present results demonstrate that the injection barrier for electrons from the Au electrode is higher in the LS/edge-on than in the spin-coated/face-on films. These data allow us to conclude that the high mobilities reported for the face-on oriented P(NDI2OD-T2) films reflect not only the efficient interchain transport in the three dimensions but also a more favorable charge injection from the gold electrode.

CONCLUSIONS

In conclusion, we have studied the energy level alignment and the activation energy for charge transport of well-ordered edge-on oriented P(NDI2OD-T2) monolayers and multilayers. The results from inverse photoemission spectroscopy measurements demonstrate that the injection barrier for electrons is higher in the LS/edge-on than in the spin-coated/face-on films, emphasizing the role of the molecular orientation at the semiconductor/contact interface in shifting the injection barrier. Contact resistances up to 1 order of magnitude higher are extracted for the edge-on oriented P(NDI2OD-T2) OFETs when compared to the face-on oriented devices. This is also revealed by variable-temperature electrical measurements disclosing higher activation energy for the edge-on-oriented backbones versus that of face-on oriented P(NDI2OD-T2) bulk films, which showed a weaker temperature dependence. Finally, we demonstrate that the high mobilities reported for the face-on oriented P(NDI2OD-T2) films, both in plane and out of plane, reflect not only efficient interchain transport in the three dimensions but also a favorable electron injection from the electrodes.

EXPERIMENTAL METHODS

P(NDI2OD-T2) was synthesized as reported by Yan et al.[6] Ordered thin films were prepared by Langmuir-Schäfer (LS) technique on glass substrates. Ultrapure Millipore water with resistivity greater than 18.2 MΩ cm was used as subphase at 25 °C. The substrates were sonicated for 10 min each in acetone, ethanol and isopropyl alcohol, and dried with nitrogen just before film growth. Prior to deposit, glass substrates were modified with hexamethyldisilazane (HMDS) after 10 min UV-ozone treatment. Films were grown from ~0.2 mg mL^{-1} P(NDI2OD-T2) in chloroform. Approximately 400 μL of solution was randomly spread onto the aqueous subphase (NIMA apparatus). After solvent evaporation, the film floating at the air/water interface was compressed continuously at a rate of 6 mm min^{-1}. The surface pressure (π) was monitored by a Wilhelmy balance. Deposition was carried out at a surface pressure of 20 mN m^{-1}, by approaching the substrate horizontally to the air/water interface. The LS polymeric films were then left drying in a vacuum oven at 150 °C overnight.

Details about the near-ultraviolet inverse photoemission spectroscopy (NUV-IPES) setup are described elsewhere.[39] A quartz glass plate coated with indium tin-oxide (ITO) with the thickness of 20 nm was used as a substrate. The HMDS and P(NDI2OD-T2) layers were prepared as mentioned above. The sample specimen was introduced into the vacuum chamber evacuated to 2×10^{-7} Pa and incident to an electron beam. To avoid the sample damage, the kinetic energy of incident electrons was restricted to less than 2.5 eV and the electron current densities ranged between 1×10^{-6} and 1×10^{-5} A cm^{-2}. Under these experimental conditions, the same IPES spectra were obtained after several scans, confirming the sample damage was negligible. The emitted photons were collected and focused into a photon detector consisting of an optical bandpass filter and a photomultiplier tube. The center wavelength and bandwidth of the bandpass filter were 285 and 14 nm, respectively. The Fermi level was determined as the onset energy of the Ag surface. The overall energy resolution was estimated to be 0.33 eV. In determining the electron affinities, the resolution was taken into account. The low energy electron transmission (LEET) spectroscopy was carried out on the same apparatus and sample films as the IPES. The electron current $I(E_k)$ was measured as a function of electron kinetic energy E_k and the LEET spectrum was obtained as the first derivative $dI(E_k)/dE_k$. The peak corresponds to the vacuum level of the sample. The vacuum level shift between the Au substrate and the spin-coated P(NDI2OD-T2) layer was measured by Kelvin Probe in air using McAllister Technical Service KP6500.

For the device preparations, thoroughly cleaned glass slides with prepatterned Cr/Au contacts (L = 50 μm, W = 500 μm) were used as substrates. Monolayer and multilayers of P(NDI2OD-T2) were transferred by LS deposition as described above and then thermally annealed in a vacuum oven overnight to fully remove the water. PMMA (Sigma-Aldrich) with M_w = 120 kg mol^{-1} was spin-coated from a solution in ethyl acetate (70 mg mL^{-1}, filtered with a 0.45 μm PTFE filter) in air at 1500 rpm for 30 s. After the dielectric deposition, the devices were annealed in vacuum oven at 150 °C for 2h. Silver top gate electrode was thermally evaporated at the final thickness of 80 nm. Electrical measurement were performed in vacuum by using a homemade vacuum probe station connected to a Keithley 4200-SCS semiconductor parameter analyzer.

AUTHOR INFORMATION

Corresponding Author

*E-mail: yoshida@e.kuicr.kyoto-u.ac.jp (H.Y.); afacchetti@polyera.com (A.F.); m.a.loi@rug.nl (M.A.L.).

Present Address

†S.F. is currently at Organic Electronics, Department of Science and Technology, Linköping University, SE-601 74 Norrköping, Sweden

Notes

The authors declare no competing financial interest.

ACKNOWLEDGMENTS

S.F. and M.A.L. thank Prof. Petra Rudolf for kindly allowing the use of Langmuir-Schäfer setup. Alessandro Luzio (IIT, Milano) is acknowledged for helpful discussions on contact resistance measurements. This work was partially supported by JST, PRESTO.

REFERENCES

(1) Arias, A. C.; MacKenzie, J. D.; McCulloch, I.; Rivnay, J.; Salleo, A. *Chem. Rev.* **2010**, *110*, 3−24.

(2) Usta, H.; Facchetti, A.; Marks, T. J. *Acc. Chem. Res.* **2011**, *44*, 501−510.

(3) Nougaret, L.; Happy, H.; Dambrine, G.; Derycke, V.; Bourgoin, J. P.; Green, A. A.; Hersam, M. C. *Appl. Phys. Lett.* **2009**, *94*, 243505.

(4) Facchetti, A. *Chem. Mater.* **2011**, *23*, 733−758.
(5) McCulloch, I.; Ashraf, R. S.; Biniek, L.; Bronstein, H.; Combe, C.; Donaghey, J. E.; James, D. I.; Nielsen, C. B.; Schroeder, B. C.; Zhang, W. M. *Acc. Chem. Res.* **2012**, *45*, 714−722.
(6) Yan, H.; Chen, Z.; Zheng, Y.; Newman, C.; Quinn, J. R.; Dötz, F.; Kastler, M.; Facchetti, A. *Nature* **2009**, *457*, 679−686.
(7) Casado, J.; Ortiz, R. P.; Navarrete, J. T. L. *Chem. Soc. Rev.* **2012**, *41*, 5672−5686.
(8) Silvestri, F.; Marrocchi, A.; Seri, M.; Kim, C.; Marks, T. J.; Facchetti, A.; Taticchi, A. *J. Am. Chem. Soc.* **2010**, *132*, 6108−6123.
(9) Zen, A.; Pflaum, J.; Hirschmann, S.; Zhuang, W.; Jaiser, F.; Asawapirom, U.; Rabe, J. P.; Scherf, U.; Neher, D. *Adv. Funct. Mater.* **2004**, *14*, 757−764.
(10) Piliego, C.; Jarzab, D.; Gigli, G.; Chen, Z.; Facchetti, A.; Loi, M. A. *Adv. Mater.* **2009**, *21*, 1573−1576.
(11) Salleo, A.; Kline, R. J.; DeLongchamp, D. M.; Chabinyc, M. L. *Adv. Mater.* **2010**, *22*, 3812−3838.
(12) Fabiano, S.; Wang, H.; Piliego, C.; Jaye, C.; Fischer, D. A.; Chen, Z. H.; Pignataro, B.; Facchetti, A.; Loo, Y. L.; Loi, M. A. *Adv. Funct. Mater.* **2011**, *21*, 4479−4486.
(13) Sirringhaus, H.; Brown, P. J.; Friend, R. H.; Nielsen, M. M.; Bechgaard, K.; Langeveld-Voss, B. M. W.; Spiering, A. J. H.; Janssen, R. A. J.; Meijer, E. W.; Herwig, P.; de Leeuw, D. M. *Nature* **1999**, *401*, 685−688.
(14) Duhm, S.; Heimel, G.; Salzmann, I.; Glowatzki, H.; Johnson, R. L.; Vollmer, A.; Rabe, J. P.; Koch, N. *Nat. Mater.* **2008**, *7*, 326−332.
(15) Heimel, G.; Salzmann, I.; Duhm, S.; Rabe, J. P.; Koch, N. *Adv. Funct. Mater.* **2009**, *19*, 3874−3879.
(16) Salzmann, I.; Duhm, S.; Heimel, G.; Oehzelt, M.; Kniprath, R.; Johnson, R. L.; Rabe, J. P.; Koch, N. *J. Am. Chem. Soc.* **2008**, *130*, 12870−12871.
(17) Hamadani, B. H.; Corley, D. A.; Ciszek, J. W.; Tour, J. M.; Natelson, D. *Nano Lett.* **2006**, *6*, 1303−1306.
(18) Fabiano, S.; Musumeci, C.; Chen, Z. H.; Scandurra, A.; Wang, H.; Loo, Y. L.; Facchetti, A.; Pignataro, B. *Adv. Mater.* **2012**, *24*, 951−956.
(19) Rivnay, J.; Toney, M. F.; Zheng, Y.; Kauvar, I. V.; Chen, Z.; Wagner, V.; Facchetti, A.; Salleo, A. *Adv. Mater.* **2010**, *22*, 4359−4363.
(20) Steyrleuthner, R.; Schubert, M.; Howard, I.; Klaumunzer, B.; Schilling, K.; Chen, Z. H.; Saalfrank, P.; Laquai, F.; Facchetti, A.; Neher, D. *J. Am. Chem. Soc.* **2012**, *134*, 18303−18317.
(21) Steyrleuthner, R.; Schubert, M.; Jaiser, F.; Blakesley, J. C.; Chen, Z.; Facchetti, A.; Neher, D. *Adv. Mater.* **2010**, *22*, 2799−2803.
(22) Rivnay, J.; Steyrleuthner, R.; Jimison, L. H.; Casadei, A.; Chen, Z.; Toney, M. F.; Facchetti, A.; Neher, D.; Salleo, A. *Macromolecules* **2011**, *44*, 5246−5255.
(23) Noh, Y. Y.; Cheng, X. Y.; Tello, M.; Lee, M. J.; Sirringhaus, H. *Semicond. Sci. Technol.* **2011**, *26*, 034003.
(24) Braga, D.; Horowitz, G. *Adv. Mater.* **2009**, *21*, 1473−1486.
(25) Baeg, K. J.; Khim, D.; Jung, S. W.; Kang, M.; You, I. K.; Kim, D. Y.; Facchetti, A.; Noh, Y. Y. *Adv. Mater.* **2012**, *24*, 5433−5439.
(26) Natali, D.; Fumagalli, L.; Sampietro, M. *J. Appl. Phys.* **2007**, *101*, 014501.
(27) Hamadani, B. H.; Natelson, D. *Appl. Phys. Lett.* **2004**, *84*, 443.
(28) Smits, E. C. P.; Mathijssen, S. G. J.; van Hal, P. A.; Setayesh, S.; Geuns, T. C. T.; Mutsaers, K.; Cantatore, E.; Wondergem, H. J.; Werzer, O.; Resel, R.; Kemerink, M.; Kirchmeyer, S.; Muzafarov, A. M.; Ponomarenko, S. A.; de Boer, B.; Blom, P. W. M.; de Leeuw, D. M. *Nature* **2008**, *455*, 956−959.
(29) Defaux, M.; Gholamrezaie, F.; Wang, J. B.; Kreyes, A.; Ziener, U.; Anokhin, D. V.; Ivanov, D. A.; Moser, A.; Neuhold, A.; Salzmann, I.; Resel, R.; de Leeuw, D. M.; Meskers, S. C. J.; Moeller, M.; Mourran, A. *Adv. Mater.* **2012**, *24*, 973−978.
(30) Letizia, J. A.; Rivnay, J.; Facchetti, A.; Ratner, M. A.; Marks, T. J. *Adv. Funct. Mater.* **2010**, *20*, 50−58.
(31) Zhao, N.; Noh, Y. Y.; Chang, J. F.; Heeney, M.; McCulloch, I.; Sirringhaus, H. *Adv. Mater.* **2009**, *21*, 3759−3763.
(32) Caironi, M.; Bird, M.; Fazzi, D.; Chen, Z. H.; Di Pietro, R.; Newman, C.; Facchetti, A.; Sirringhaus, H. *Adv. Funct. Mater.* **2011**, *21*, 3371−3381.
(33) Sze, S. *Physics of Semiconductor Devices*, 3nd ed.; Wiley: New York, 2006; p 154.
(34) Blakesley, J. C.; Schubert, M.; Steyrleuthner, R.; Chen, Z. H.; Facchetti, A.; Neher, D. *Appl. Phys. Lett.* **2011**, *99*, 183310.
(35) Wu, C. I.; Hirose, Y.; Sirringhaus, H.; Kahn, A. *Chem. Phys. Lett.* **1997**, *272*, 43−47.
(36) Frank, K. H.; Dudde, R.; Koch, E. E. *Chem. Phys. Lett.* **1986**, *132*, 83−87.
(37) Sato, N.; Yoshida, H.; Tsutsumi, K. *J. Electron Spectrosc. Relat. Phenom.* **1998**, *88*, 861−865.
(38) Tsutsumi, K.; Yoshida, H.; Sato, N. *Chem. Phys. Lett.* **2002**, *361*, 367−373.
(39) Yoshida, H. *Chem. Phys. Lett.* **2012**, *539*, 180−185.
(40) Chen, Z. H.; Zheng, Y.; Yan, H.; Facchetti, A. *J. Am. Chem. Soc.* **2009**, *131*, 8−9.
(41) Ishii, H.; Sugiyama, K.; Ito, E.; Seki, K. *Adv. Mater.* **1999**, *11*, 605−625.
(42) Braun, S.; Salaneck, W. R.; Fahlman, M. *Adv. Mater.* **2009**, *21*, 1450−1472.
(43) Lange, I.; Blakesley, J. C.; Frisch, J.; Vollmer, A.; Koch, N.; Neher, D. *Phys. Rev. Lett.* **2011**, *106*, 216402.